Molecular Dynamics Simulations of 1,2-Dimethoxypropane and 1,2-Dimethoxyethane in Aqueous Solution

Dmitry Bedrov and Grant D. Smith*

Department of Chemical and Fuels Engineering and Department of Materials Science and Engineering, University of Utah, 122 South Central Campus Dr., Room 304, Salt Lake City, Utah 84112

Received: May 4, 1999; In Final Form: July 7, 1999

We report on the thermodynamic properties, conformations, and local structure of aqueous solutions of 1,2-dimethoxypropane (DMP) as a function of composition and temperature as obtained from molecular dynamics simulations and compare results with simulations of aqueous solutions of 1,2-dimethoxyethane (DME). The density of DMP/water solutions was found to be systematically lower than that for DME solutions of the same composition, reflecting the lower density of neat DMP compared to DME. The excess volume of DMP/water solutions closely resembles that of DME/water solutions, indicating that the nature of DMP solvation is similar to that of DME. The magnitude and composition dependence of the self-diffusion coefficient of water and ether in the DMP/water solutions were also found to closely resemble those of DME/water solutions. As in DME/water solutions, the populations of DMP conformers with favorable dipole−dipole interactions between the ether and solvating water (i.e., hydrophilic conformers) were found to increase with increasing dilution (water content). The free energy of stabilization (relative to the respective *ttt* conformers) for hydrophilic conformers in dilute solution was found to be around 1.5 kcal/mol for both DME and DMP solutions. The local structure, e.g., pair distribution functions and extent of hydrogen bonding, is similar for the more dilute DMP and DME solutions. However, the intrinsically higher conformational energy of the hydrophilic DMP conformers results in a much lower fraction of these conformers for all solution compositions compared to DME solutions. At higher ether content, this leads to significantly greater clustering of water molecules in DMP solutions and is probably the principal reason for the disparate phase behavior seen for poly(ethylene oxide) and poly(propylene oxide).

Introduction

Poly(ethylene oxide) (PEO) and poly(propylene oxide) (PPO) are widely employed in a variety of applications involving interactions with an aqueous environment. Despite similarity in molecular structure, the phase behavior of these polymers in aqueous solution differs significantly. Only short PPO oligomers (molecular weight < 400 Da) are soluble in water,[1] while PEO shows complete miscibility for all molecular weights at room temperature.[2] In this paper we will explore the physical reasons for the disparate phase behavior of these polymers by comparing properties of 1,2-dimethoxypropane (DMP) (the PPO shortest oligomer) and 1,2-dimethoxyethane (DME) (the PEO shortest oligomer) in aqueous solutions as determined from molecular dynamics (MD) simulations.

In our previous work we developed an atomistic description of DME/water[3] as well as DMP/water[4] interactions. These atomistic force fields were parametrized to reproduce the geometries and energies of DME/water and DMP/water clusters determined from high-level ab initio calculations, while employing quantum chemistry based potentials for DMP[4] and DME[5] and the TIP4P (four-point transferable intermolecular potential) model for water.[6] Previously we performed molecular dynamics simulations of DME in aqueous solution as a function of solution composition and temperature. Thermodynamic properties of the solutions were found to be in a good agreement with experiment.[3] The conformational,[7] structural,[7] and dynamic[8,9] properties of DME/water solutions as a function of concentration and temperature from molecular dynamics simulations were also investigated.

In this paper we compare results of simulations of DMP/water solutions with those of DME/water solutions. We discuss similarities and differences in thermodynamic, conformational, structural, and dynamic properties of the solutions as a function of composition and temperature. From these comparisons we are able to infer the reasons for the dissimilar phase behavior of PEO and PPO in aqueous solutions.

Molecular Dynamics Simulation Force Field and Methodology

A detailed description of the atomistic force fields for the DME (PEO)/water and DMP (PPO)/water systems are given in refs 3 and 4, respectively. In this work we perform simulations using the constant temperature/pressure methods[10] implemented as described elsewhere.[11] Five DMP/water and DME/water systems with mole fraction of ether $X_{ether} = 0.04$, 0.10, 0.18, 0.42, and 0.72 were investigated. Simulations were performed at 318 K and an average pressure about 1 atm. For $X_{ether} = 0.04$ and 0.18 simulations at 368 K were also performed in order to establish the temperature dependence of the solution properties. Periodic boundary conditions were employed. The standard Shake algorithm[12] was used to constrain the bond length, while all other degrees of freedom remained flexible. The Ewald summation method[13] was employed to handle long-range electrostatic interactions. The initial systems, consisting of DMP (or DME) and water molecules in a regular array with a greatly reduced density, were equilibrated for 0.1 ns. The density was increased over 0.5 ns until the pressure reached 1 atm. Each system was then equilibrated over 2 ns. Sampling for each

10.1021/jp991454p CCC: $18.00
Published on Web 10/22/1999

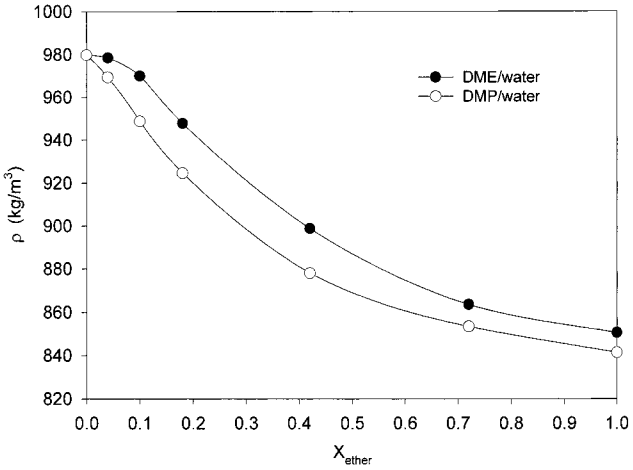

Figure 1. Densities of DME and DMP solutions as a function of ether mole fraction at 318 K.

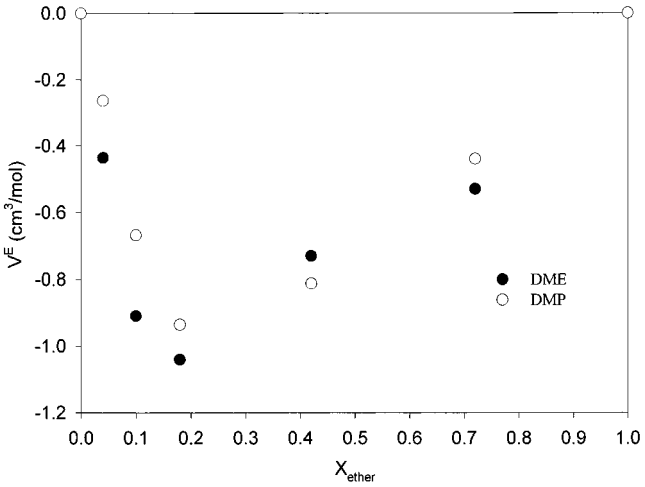

Figure 2. Solution excess volume for DME and DMP solutions as a function of ether mole fraction at 318 K.

system occurred over 1.0−3.0 ns (depending on composition) with a time step of 1.0 fs. Each system contained about 1300 atoms, and all systems contained at least 10 ether molecules.

Thermodynamic Properties

In Figure 1 we show the composition dependence of the densities of the DMP/water and DME/water solutions. The solution densities are qualitatively similar, showing negative deviation from ideal mixture behavior for both ethers. For all compositions the DMP solutions have a lower density than the corresponding DME solution, reflecting the intrinsic lower density of neat DMP in comparison with neat DME.[14] The solution excess volumes, which quantify deviation from ideal solution behavior, are shown in Figure 2. Both solutions show a minimum (largest negative value) in excess volume around $X_{\text{ether}} \sim 0.20$. The similarity in the solution properties of the ethers is further supported by Figure 3, where the self-diffusion coefficients of ethers and water molecules as a function of solution composition at 318 K are presented. All self-diffusion coefficients have a minimum at mole fraction $X_{\text{ether}} \sim 0.2$. A detailed explanation of this behavior can be found in ref 8. For the water self-diffusion coefficient in DME solutions, excellent agreement between simulation and experiment was seen.[9]

Conformational Properties

Relative Free Energies. In Table 1 we show the populations for the major DMP and DME conformers at 318 K as a function of solution composition. In Table 2 we compare the relative free energies of the important DME and DMP conformers for $X_{\text{ether}} = 0.04$ at 318 K. The relative (to the respective *ttt* conformer) conformer free energies were determined using the relationship

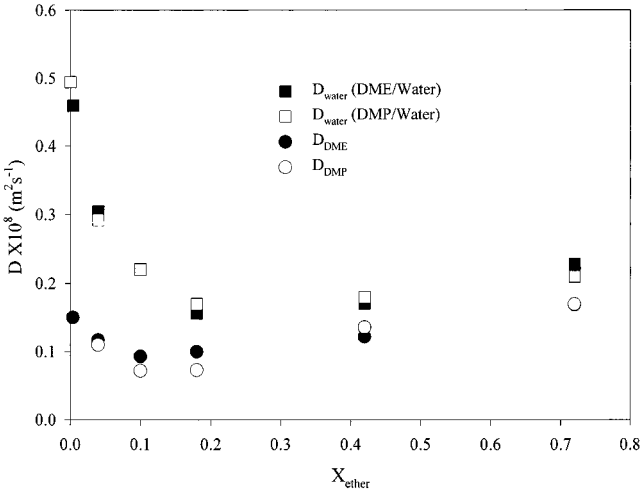

Figure 3. Self-diffusion coefficients of ether and water for DME and DMP solutions as a function of ether mole fraction at 318 K.

TABLE 1: Populations of DMP and DME Conformers as a Function of Composition at 318 K

	X_{ether}					
conformer[a]	0.04[b]	0.10	0.18	0.42	0.72	1.00
	DMP					
ttt	5.9 (6.4)	5.4	7.6 (7.3)	11.5	15.4	17.6
tgt	25.7 (19.5)	23.9	18.1 (13.8)	16.0	14.6	13.0
$t\bar{g}t$	22.1 (23.0)	23.0	26.5 (25.2)	18.3	13.1	10.4
gtt	5.0 (6.0)	5.4	6.1 (6.5)	9.4	11.6	13.3
ggt	7.9 (7.9)	8.7	7.8 (8.1)	12.9	16.2	18.0
$g\bar{g}t$	19.7 (19.1)	19.8	20.9 (21.1)	15.0	10.3	8.0
tgg	4.2 (4.6)	3.9	2.9 (2.8)	2.7	2.0	1.5
hydrophilic fraction	71.7 (66.2)	70.6	68.4 (62.9)	52.0	40.0	32.9
	DME					
ttt	3.3 (5.2)	3.7	5.3 (7.0)	7.5	11.0	17.7
tgt	70.7 (60.9)	70.5	65.1 (54.7)	56.7	49.3	44.9
ttg	2.5 (4.3)	2.3	3.2 (5.1)	4.9	6.2	9.1
tgg	15.9 (15.5)	15.0	15.4 (14.9)	12.8	11.1	8.1
tg^+g^-	5.5 (10.4)	6.5	8.9 (13.6)	14.2	16.1	17.2
hydrophilic fraction	86.6 (76.4)	85.5	80.5 (69.6)	69.5	60.4	53.0

[a] Includes all conformers with >2% population for $X_{\text{ether}} = 0.04$ solutions. [b] Numbers in parentheses are at 368 K.

TABLE 2: Relative Free Energies of DMP and DME Conformers for $X_{\text{ether}} = 0.04$

conformer[a]	ΔA[b]	ΔA_i(gas phase)	$\Delta\Delta A$
	DMP		
ttt **[0.4]**	0.00	0.00	0.00
tgt **[1.3]**	**−0.92 (−0.81)**	**0.50**	**−1.42**
tḡt **[1.8]**	**−0.83 (−0.93)**	**0.97**	**−1.80**
gtt [1.6]	0.11 (0.05)	0.21	−0.10
ggt [1.6]	−0.18 (−0.15)	0.05	−0.23
gḡt [2.7]	**−0.76 (−0.79)**	**1.15**	**−1.91**
tgg **[1.3]**	**0.25 (0.23)**	**2.03**	**−1.78**
	DME		
ttt [0.0]	0.00	0.00	0.00
tgt **[1.5]**	**−1.49 (−1.29)**	**0.30**	**−1.79**
tg^+g^- [1.7]	0.55 (0.51)	0.70	−0.15
tgg **[2.7]**	**−0.11 (0.2)**	**1.80**	**−1.91**

[a] Numbers in brackets are conformer dipole moments in debyes [ref 19]. [b] Free energies are in kcal/mol. Numbers in parentheses are at 368 K. Hydrophilic conformers (see text) are in bold.

$$\Delta A_i = kT \ln \frac{d_i f_{ttt}}{f_i} \tag{1}$$

Here, i denotes a particular conformer, T is temperature, d_i is the degeneracy of the conformer, and f_i is the conformer population (from Table 1). Uncertainties in the populations and free energies were determined as follows. For a given composition, a trajectory of length t_{sim} can be divided into N subtrajectories of length t_{sim}/N. If the subtrajectories are sufficiently long, then the average conformer populations for each subtrajectory are statistically independent, and the variance in population for each conformer i is given by standard random error analysis as

$$\delta P_i = \sqrt{\frac{\sum_{j=1}^{N} [P_{ij} - \langle P_i \rangle]^2}{N-1}} / \sqrt{N} \tag{2}$$

where P_i is the population of conformer i, P_{ij} is the jth measurement of P_i, i.e., the mean of P_i in the jth subtrajectory, and $\langle P_i \rangle$ is the mean of P_i over the length of the total trajectory. By plotting δP_i as a function of N, it is possible to determine the length of the subtrajectory required to obtain independent "measurements". We find that 50 ps (the torsional autocorrelation time is approximately 2 ps[8]) subtrajectories yield independent populations. From eq 1, the variance in relative free energies is given by

$$\delta \Delta A_i = kT \left[\left| \frac{\delta P_{ttt}}{P_{ttt}} \right| + \left| \frac{\delta P_i}{P_i} \right| \right] \tag{3}$$

The variance in population was found to be less than 0.01 for all conformers reported in Table 1, and the variance in relative free energies was less than 0.1 kcal/mol for all conformers reported in Table 2.

The strength of the interaction of the ether with water as a function of conformation was determined by subtracting the gas-phase values of the relative free energies from the solution values, or

$$\Delta\Delta A_i = \Delta A_i - \Delta A_i(\text{gas phase}) \tag{4}$$

The gas-phase relative free energy differences ΔA_i(gas phase) reflect the inherent differences in free energies of the conformers as determined from gas-phase molecular dynamics simulations. Hence $\Delta\Delta A_i$ is a measure of the relative (to *ttt*) interaction of a conformer with water. Values of $\Delta\Delta A_i$ at 318 K for DMP and DME conformers are also presented in Table 2. It can be seen that the *tgt*, *tḡt*, *gḡt* and *tgg* DMP conformers have relatively favorable interactions with water: the large, negative $\Delta\Delta A_i$ values for these conformers reflect the dramatic increase in their populations in aqueous solution compared to the gas phase. We classify these, as well as the DME *tgt* and *tgg* conformers, as "hydrophilic" and the remaining DMP and DME conformers as "hydrophobic". The similarity in $\Delta\Delta A_i$ values for the hydrophilic DMP and DME conformers implies that water stabilizes the hydrophilic DMP and DME conformers equally well *relative to the respective ttt conformers*. We will return to this latter point below.

Comparing the populations of the DMP and DME conformers from Table 1, a significant difference in the total population of hydrophilic conformers for the two ethers can be observed. This fraction is given in Table 1. This difference is due, to a large extent, to the intrinsic lower population of hydrophilic conformers in DMP. This is reflected in the ΔA_i(gas phase) values given in Table 2. In other words, the hydrophilic conformers of DMP are higher in intrinsic conformational energy (relative to the hydrophobic *ttt* conformer) than those of DME.

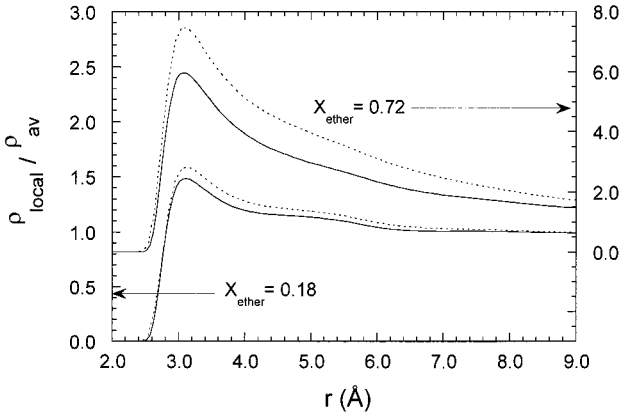

Figure 4. Ratio of the local water density (water coordination number per unit volume in a sphere of radius r from a given water molecule) to the bulk solution density of water at 318 K. Solid curves are for DME solutions while dashed curves are for DMP solutions.

Composition Dependence. Table 1 reveals that for both ethers the fraction of hydrophilic conformers decreases with increasing ether concentration. We showed in previous studies of DME solutions that, with increasing ether concentration, there is a tendency of hydrophobic conformers to interact with other hydrophobic conformers, while the hydrophilic conformers prefer to interact with water. With increasing ether content, the fraction of hydrophobic conformers increases and the preference of ether−ether and water−water contacts over interspecies contacts increases. This behavior is consistent with the water clustering seen in more concentrated ether solutions, illustrated in Figure 4. As DMP has an intrinsically higher fraction of hydrophobic conformers, we would expect the degree of water clustering in DMP solutions to be greater than in DME solutions. This is indeed the case, as illustrated in Figure 4.

While the conformational populations of DMP solutions show qualitatively the same composition dependence as seen in DME solutions, there are some features of this dependence that are not manifested in DME solutions. Specifically, several of the important DMP conformers (*tḡt*, *gḡt* and *gtt*) exhibit an extremum in their populations in the composition range $X_{DMP} = 0.1-0.2$. The extremum is especially pronounced for the *tḡt* *gḡt* and conformers. Both of these conformers have a $\bar{g}$ orientation of the −O−C−C−O− dihedral, and therefore, the behavior of the populations of these conformers could be due to some particular interaction between water molecules and DMP conformers with a $\bar{g}$ orientation for the central dihedral. In Figure 5 we show the *tgt* and *tḡt* conformers of DMP. It can be seen that for the *tgt* conformer the α-methyl group is rotated away from ether oxygen atom, while for the *tḡt* the α-methyl group has very strong interaction with one of the ether oxygen atoms. The water molecules hydrating DMP also prefer to interact with the DMP oxygen atoms. We find, as in DME, that the number of hydrogen bonds formed between water and DMP is nearly independent of the DMP conformer. Hence, as was found for DME, the relative stabilization of particular DMP conformers is due primarily to favorable dipole−dipole DMP−water and water−water interactions involving the ether and its first hydration shell of water. Additional water molecules must adjust their orientation in the DMP hydration shell in order to

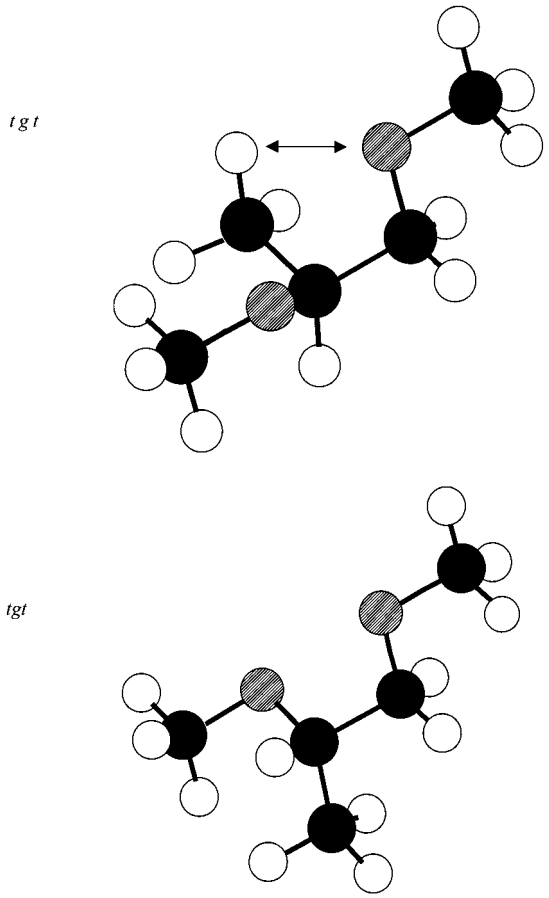

Figure 5. The *tgt* and *tḡt* conformers of DMP.

accommodate both DMP and its hydrating molecules. For conformers with a $\bar{g}$ orientation of the central dihedral, the α-methyl group imposes restrictions on the available positions and orientations for these added water molecules not present in the other hydrophilic conformers. Similar conformational behavior with extremum in composition dependence was observed experimentally[15] and later explained by simulation[16] for some conformers of short PEO oligomers larger than DME. The effect was explained in terms of unfavorable dipole−dipole interactions of water molecules completing the hydration shell of the oligomer with other neighboring dipoles.

Conformer Classification and Mean-Field Models. In application of mean-field models to PEO[17] and PPO[18] solutions, ether conformations are classified as hydrophobic or hydrophilic. The nonpolar conformers (those with no or small dipole moments) are considered hydrophobic, while the polar conformers are considered hydrophilic. Table 2 reveals that a large dipole moment[19,20] does not necessarily result in conformer hydrophilicity. For example, the tg^+g^- DME and *ggt* DMP conformers have relatively large dipole moments but belong to the hydrophobic class. The correlation in orientations of water molecules comprising the first hydration shell with the ether dipole moment and the dipole moments of the other hydrating waters is more important for stabilization of particular conformers in aqueous solution than the actual value of the dipole moment. Moreover, as in case for the *tḡt* and *gḡt* DMP conformers, hydrophilicity can be a composition-dependent property. Therefore, we believe that while the two-state models of PEO and PPO solutions can capture some features of the phase behavior in these systems, they do not lead to correct description of polymer conformations and provide an incomplete picture of the driving forces for the phase separation.

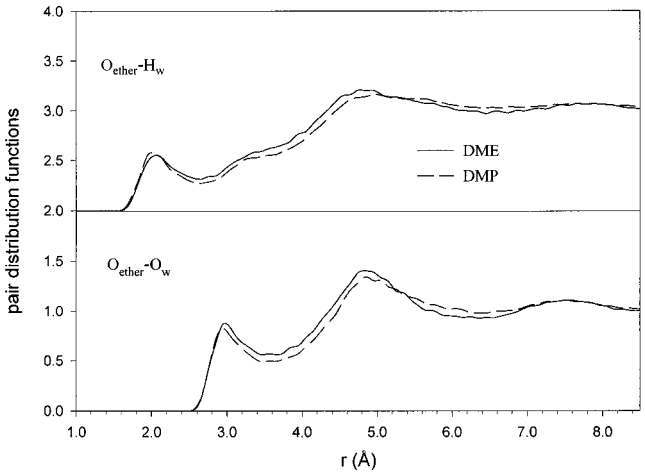

Figure 6. $O_{ether}-H_{water}$ and $O_{ether}-O_{water}$ pair distribution functions at $X_{ether} = 0.04$ at 318 K. The $O_{ether}-H_{water}$ values have been offset by 2.

Temperature Dependence. In Table 1 the conformational populations of the DMP and DME conformers at 368 K are shown in parentheses for compositions $X_{ether} = 0.04$ and 0.18. For $X_{ether} = 0.04$, the relative free energies ΔA at 368 K are given in Table 2. Table 2 reveals that for both ethers the relative free energies are not very temperature dependent for $X_{ether} = 0.04$. This allows us to assume that the *relative* stabilization of particular conformers in dilute solution is mostly due to the difference in enthalpy of solvation of the conformers and not due to entropy differences. For more concentrated solutions, the picture is somewhat different. Our previous work with DME revealed an entropic contribution to the relative free energies of solvation, which we associated with the number of water molecules "perturbed" by each class of conformer. Hydrophobic conformers tend to interact with each other, and hence perturb less water than hydrophilic conformers, which are more thoroughly solvated. This solvation is an entropically unfavorable process; hence for more concentrated solutions the free energy of solvation for hydrophilic conformers becomes less favorable with increasing temperature.

It is also worth noting that the maximum in population of the DMP *tḡt* conformer at 368 K with composition is less pronounced than was found at 318 K. This means that the effects that are destabilizing the DMP *tḡt* conformer in dilute solutions disappear with increasing temperature. The explanation of the destabilization of the DMP *tḡt* conformer in dilute solutions given above is consistent with such temperature behavior. At higher temperatures the correlations between orientations of water molecules decreases and, therefore, interference of the α-methyl group becomes less important.

Local Structure

Interspecies Pair Distribution Functions. The $O_{ether}-H_w$ and $O_{ether}-O_w$ pair distribution functions in DMP and DME solutions for $X_{ether} = 0.04$ are shown in Figure 6 at 318 K. The $O_{ether}-O_w$ pair distribution functions reveals that the DMP oxygen atom on average has slightly fewer water molecules in its first and second hydration shells than DME oxygen, due to replacement of several water molecules in the ether hydration shell by the pendent methyl group. Similar behavior was seen for $X_{ether} = 0.18$ solutions. The number of hydrogen bonds (defined as the integral of the first peak in the $O_{ether}-H_w$ pair distribution function) was found to be nearly identical for DME and DMP for all solution concentrations. Therefore the extent of hydrogen bonding is independent of ether type and is unlikely

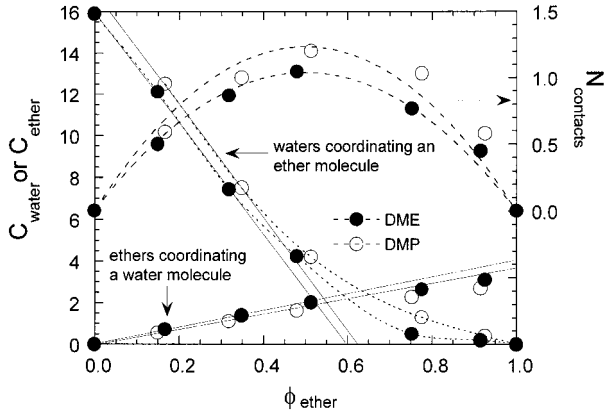

Figure 7. Water and ether coordination numbers (left ordinate) and number of interspecies contacts per molecule (right ordinate) for DME and DMP solutions as a function of ether volume fraction at 318 K. Dashed lines are a fit of eq 6 to the number of interspecies contacts. Solid lines are linear fits to the dilute solution data. Dotted lines are to guide the eye.

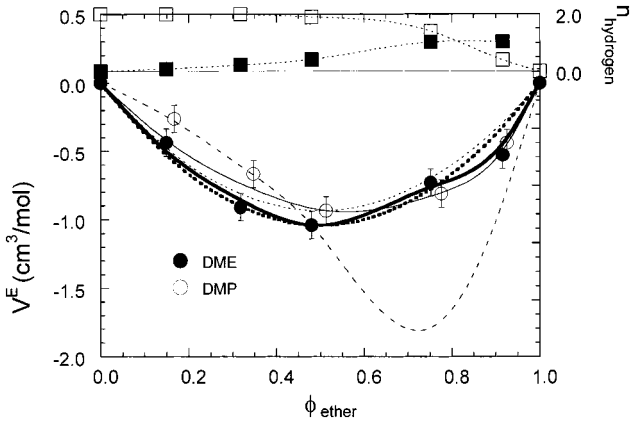

Figure 8. Solution excess volume for DME and DMP solutions as a function of ether volume fraction at 318 K. The solid lines (heavy = DME, light = DMP) assume that the excess volume is proportional to the number of interspecies contacts as determined from simulation, while the corresponding dotted lines assume that the number of interspecies contacts is given by the random mixing model. The dashed line (DME) assumes that the excess volume is proportional to the number of interspecies hydrogen bonds. In all cases, the proportionality constants were determined by matching the minimum (most negative) excess volume. Shown on the right ordinate is the number of hydrogen bonds per DME molecule (open squares) and number of hydrogen bonds per water molecule (filled squares).

to be an explanation for differences in solubility of PPO and PEO molecules. However, for more concentrated solutions differences are seen between DME and DMP for the interspecies (ether−water) pair distribution function. For example, this is reflected in the greater water clustering seen in the DMP solutions $X_{ether} = 0.72$ compared to DME, as illustrated in Figure 4.

Interspecies Interactions. It is of interest to investigate the concentration dependence of the coordination of ether and water in greater detail. Assuming random mixing of ether and water molecules in the solutions, the number of water molecules coordinating an ether molecule is proportional to the volume fraction of water ϕ_w while the number of ether molecules coordinating a water molecule is proportional to the volume fraction of ether ϕ_{ether}. Figure 7 shows the number of water molecules in the first coordination shell[21] of DME and DMP as well as the number of ethers coordinating a water molecule as a function of solution composition. For the more dilute solutions, the composition dependence does appear to be linear as expected from the random-mixing assumption. For higher ether concentrations, deviation from random-mixing behavior is seen, consistent with the clustering of water molecules illustrated in Figure 4. Analogous clusters of ether molecules in dilute solutions are not seen.

The number of interspecies (ether−water) contacts is given as

$$N_{contacts}(\phi_{ether}) = 0.5[X_{ether}C_{water} + (1 - X_{ether})C_{ether}] \quad (5)$$

where the number of waters coordinating an ether (C_{water}) and the number of ethers coordinating a water (C_{ether}) are taken from Figure 7. For random mixing

$$N_{contacts}(\phi_{ether}) = K\phi_{ether}\phi_{water} \quad (6)$$

where K is a proportionality constant. The number of interspecies contacts from eq 5 is shown in Figure 7 for both DMP and DME solutions. A fit of eq 6 to these results indicates that the random-mixing model does a reasonable job in describing the total number of interspecies contacts. Larger deviations are seen for the DMP solutions, where water clustering is greater.

If we assume that the excess volume (Figure 2) is proportional to the number of interspecies contacts, given in Figure 7, a good description of the excess volume can be obtained as shown in Figure 8. Taking the number of interspecies contacts from the random-mixing model yields a less satisfactory representation. If we try to relate the excess volume to the number of hydrogen bonds, a very poor description is obtained, as illustrated in Figure 8.

Conclusions

Comparison of the thermodynamic and structural properties of DMP and DME in aqueous solution reveals a strong similarity between the two solutions. Differences in local structure are small for more dilute solutions, while the degree of hydrogen bonding is similar for all solution compositions. For both solutions, conformers can be classified as hydrophobic or hydrophilic on the basis of their relative interactions with water, which depend on differences in dipole−dipole interactions in the vicinity of particular conformers. For dilute solutions, the free energy of stabilization of the hydrophilic conformers is quite similar for DMP and DME solutions.

The most dramatic difference between DMP and DME solutions is in the total population of the hydrophilic conformers. The fraction is significantly lower in DMP solutions than in the DME solutions due to an intrinsically higher conformational energy of the hydrophilic DMP conformers in comparison with major hydrophobic conformers. The higher fraction of hydrophobic conformers in DMP solutions is associated with increased water clustering in more concentrated solutions compared to DME solutions.

From the above, we might conclude that differences in the interaction of DMP and DME with water (and hence differences in the phase behavior of PPO and PEO in aqueous solution) are due almost entirely to the intrinsically lower population of hydrophilic conformations of DMP and hence PPO. We believe that this is an important, and probably the most important, difference between the two ethers and their polymers. However, we must realize that the similar stabilization of hydrophilic conformers of DME and DMP seen in Table 2 reflects interactions of water with these conformers *relative* to the respective *ttt* conformers. What is not known from this analysis is whether the interactions of water with *ttt* DME and *ttt* DMP

are similar. Hence, we performed simulations of DMP and DME solutions at $X_{ether} = 0.04$ with ethers constrained to the respective *ttt* conformations. These simulations reveal that *energetically* the interactions of *ttt* DMP and *ttt* DME with water in dilute solutions cannot be differentiated within the simulation uncertainty of about 0.3 kcal/mol per ether molecule out of 8.6 kcal/mol per ether molecule.[22] Note that this is an energy difference, not a free energy difference as given in Table 2. It is possible that the entropic effects resulting from the interaction of *ttt* DMP and water are significantly different than those of *ttt* DME and water. We believe that this is unlikely given the preponderance of evidence indicating similarity in the solutions with the exception of the total hydrophilic population, which is an intrinsic molecular property. However, Figure 7 reveals that there are slightly more water molecules associated with the hydration of a DMP molecule than for a DME molecule. Hence, DMP, being a slightly larger molecule, perturbs more water, and hence may have a larger negative entropy of solvation. The entropy of solvation of DME and DMP will be addressed in a future publication.

Acknowledgment. The authors are indebted to the National Science Foundation—Division of Materials Research for support provided through Grant NSF DMR 96244.

References and Notes

(1) Malcolm, G. N.; Rowlinson, J. S. *Trans. Faraday Soc.* **1957**, *53*, 921.

(2) Saeki, S.; Kuwahara, N.; Nakata, M.; Kaneko, M. *Polymer* **1976**, *17*, 685.

(3) Bedrov, D.; Pekny, M.; Smith, G. D. *J. Phys. Chem. B* **1998**, *102*, 996.

(4) Smith, G. D.; Borodin, O.; Bedrov, D. *J. Phys. Chem. A* **1998**, *102*, 10318.

(5) Jaffe, R. L.; Smith, G. D.; Yoon, D. Y. *J. Phys. Chem.* **1993**, *97*, 12752.

(6) Jorgensen, W. L.; Chandrasekhar, J.; Madura, J. D.; Impey, R. W.; Klein, M. *J. Chem. Phys.* **1983**, *79*, 926.

(7) Bedrov, D.; Borodin, O.; Smith, G. D. *J. Phys. Chem. B* **1998**, *102*, 5683.

(8) Bedrov, D.; Borodin, O.; Smith, G. D. *J. Phys. Chem. B* **1998**, *102*, 9565.

(9) Bedrov, D.; Smith, G. D.; Trouw, F. Manuscript in preparation.

(10) Nose, S. *J. Chem. Phys.* **1984**, *81*, 511.

(11) Smith, G. D.; Jaffe, R. L.; Yoon, D. Y. *Macromolecules* **1993**, *26*, 298.

(12) Ryckaert, J., Ciccotti, G., Berendsen, H. J. C. *J. Comput. Phys.* **1977**, *23*, 327.

(13) Allen, M. P.; Tildesley, D. T. *Computer Simulation of Liquids*; Oxford: 1987.

(14) Das, B.; Roy, M. N.; Hazra, D. K. *Indian J. Chem. Technol.* **1994**, *1*, 93; Sigma-Aldrich Regulatory & Safety Data (www.sial.com), 1 (1), 213B.

(15) Matsuura, H.; Sagawa, T. *J. Mol. Liq.* **1995**, *65/66*, 313.

(16) Bedrov, D.; Smith, G. D. *J. Chem. Phys.* **1998**, *109*, 8118.

(17) Karlstrom, G. *J. Phys. Chem.* **1985**, *89*, 4962.

(18) Carlsson, M.; Hallen, D.; Linse, P. *J. Chem. Soc., Faraday Trans.* **1995**, *91*, 2081.

(19) Sasanuma, Y.; *Macromolecules* **1995**, *28*, 8629.

(20) Smith, G. D.; Jaffe, R. L.; Yoon, D. Y. *J. Am. Chem. Soc.* **1995**, *117*, 530.

(21) The first hydration shell of ether is defined as all water molecules in the vicinity of 4.0 Å from any C or O atoms of ether.

(22) This number was obtained by taking the difference in total intermolecular nonbonded energies between pure water (240 molecules) and dilute solutions (240 water molecules and 10 ether molecules constrained to the *ttt* conformation).